Check for updates

Influence of Fracture Toughness on Multi-axial Loading Interaction Criteria for Wrapped Composite Joints

Gisele Cintra[1(✉)], Mathieu Koetsier[1], Vasileios Mylonopoulos[2], and Marko Pavlovic[1]

[1] Faculty of Civil Engineering and Geoscience, Technical University Delft, 2600 AA Delft, the Netherlands
{G.Cintra,M.Koetsier,M.Pavlovic}@tudelft.nl
[2] Tree Composites B.V, Rotterdamseweg 266a, 2628 AS Delft, the Netherlands
vasileios.mylonopoulos@treecomposites.com

Abstract. Wrapped composite joints arise as an innovative solution for joining circular non-welded hollow sections (CHS) in jacket support structures for offshore wind, intending to enhance fatigue performance and consequently reduce weight and costs when compared to traditional welded joints. Due to combined wave and wind loads, these joints are subjected to different multi-axial loading scenarios. Therefore, it becomes fundamental to establish an interaction criterion that accurately predicts the failure behavior provided by the superposition of different load conditions. Preliminary analyses have shown that, for instance, in cases where axial loads act simultaneously with bending moments, the joint resistance is underestimated when considering a linear summation of normalized strength values. Therefore, further studies are needed to determine the optimum interaction criterion exponents. In this context, this paper aims to present the results of an ongoing numerical investigation on the multi-axial load behavior of wrapped composite joints. Based on previous standards, a multi-axial loading interaction criterion is proposed, and a finite-element (FE) model is developed using the cohesive zone model approach. Distinct load cases are applied in a medium-scale X-shaped wrapped joint to evaluate the influence of the fracture toughness parameter on interaction failure criteria exponents. It was concluded that the given exponents do not seem to be affected by the change of interfacial strength and fracture toughness, which represents a valuable finding for the development of future design guidelines.

Keywords: Off-shore wind · Wrapped composite joints · Multi-axial loading · Fracture toughness · Finite element modeling

1 Introduction

The current energy transition highlights the urge to expand wind farms worldwide. However, 80% of the world's offshore wind resource potential is located in waters deeper than 60 m [1], increasing the need for innovative solutions and technology development

J. R. Correia et al. (Eds.): CICE 2025, LNCE 777, pp. 524–534, 2026.
https://doi.org/10.1007/978-3-032-09399-8_50

applied to offshore structure foundations. The use of jackets for supporting large wind turbines is a very good alternative due to its less usage of steel when compared, for instance, to monopiles. Nevertheless, this type of foundation faces significant challenges related to the welded joints, which govern the structure design due to its fatigue resistance. This solution ends up leading to a less economical design due to the need to use thicker tubes to avoid fatigue failure in the welded corners [1], which are regions with high stress concentrations.

In this context, wrapped composite joints emerge as an innovative solution to connect circular non-welded hollow sections (CHS) in jacket support structures, intending to replace traditional welded joints between braces and/or chord members. The composite wrapping allows a smoother load transfer at the joints by reducing stress concentration, and therefore enhancing fatigue endurance. Consequently, this solution enables significant weight and cost reduction when compared to conventional welded joints. Previous papers have shown that, under uniaxial loading, the wrapped composite joints present higher stiffness and ultimate load-bearing resistance when compared to welded equivalents [2]. Nevertheless, it is important to highlight that these joints are often subjected to multi-axial loading when connecting the brace members, due to the action of wind and wave loads. Previous papers have reported experimental findings on the multi-axial behavior of these joints, pointing out the composite joints' remarkable bending resistance and rotation capacity prior to failure [3]. Moreover, previous experiments indicated that there is no significant change between failure modes when compared to uniaxial loading, showing that the joints presented a consistent onset of failure at the steel-composite interface, which progresses towards the wrapping end above the steel brace [3]. However, there is still a gap related to the interaction criteria for joints subjected to simultaneous axial and bending forces, especially when it concerns the exponents of the multi-axial loading interaction criterion. In order to contribute to future design guidelines and reliable failure prediction of wrapped composite joints, it is fundamental to understand the sensitivity of these exponents to fracture parameters.

This paper aims to investigate the influence of fracture toughness on the multi-axial loading criterion for wrapped composite joints. A parametric study is conducted with the aid of the cohesive zone model (CZM) approach to predict the failure of the wrapped composite joint. Six bi-axial loading cases, focusing on the combination of axial loads (N_x) and moments out-of-plane (M_{op}), are assessed and an estimate of the failure envelopes for three different fracture toughness values is obtained. Finally, the influence of the fracture parameters on the multi-axial interaction criterion exponents is evaluated and discussed.

2 Studied Material

This paper addresses the behavior of a medium-scale 90° X-joint, which is used to connect brace members in offshore structures, and presents approximately 1/4 of a typical full-scale joint. It is composed of four steel CHS tubes (two chords and two braces) with grade S355, having 168.3 mm of diameter and 12.5 mm of thickness. The steel tubes are wrapped by a composite with E-glass fibers embedded in a thermosetting vinyl ester resin, as shown in Fig. 1b, which is manufactured through a hand-lamination procedure. The steel members' thickness was intentionally over-designed in order to lead mainly to the most unknown failure mode of wrapped composite joints, which is the debonding between steel and composite.

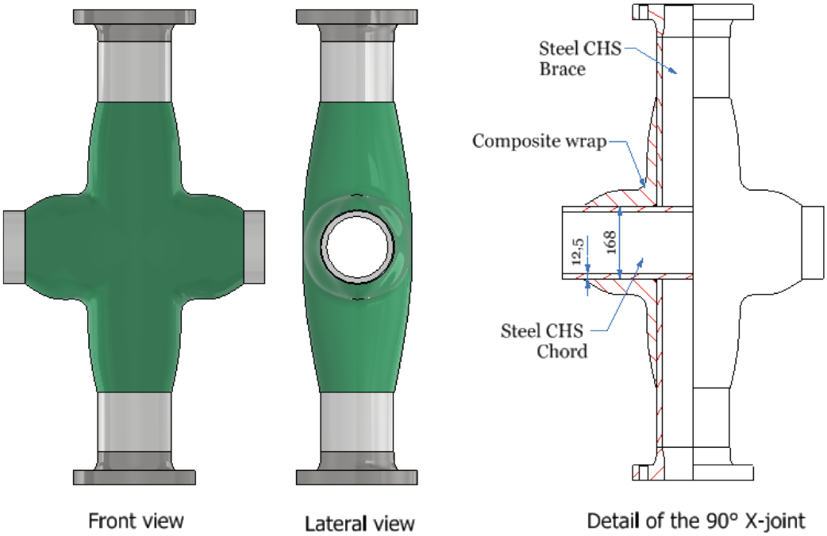

Fig. 1. Overview and detail of the studied 90° X-join

3 Numerical Analysis

3.1 Material Properties

The joint is simulated numerically in a 3D stress finite element model (FEM) using Abaqus/Explicit 2023 v.6.26 [4] to optimize convergence issues. Shrinkage due to the polymeric resin cure process is taken into account by imposing a homogeneous temperature on the wrap geometry. The elastic material properties were calibrated based on previous experiments [5], and the anisotropic yielding behavior of the composite wrap component is taken into account. On the other hand, for steel tubes, plasticity is disregarded to prevent steel from yielding and to separate the failure due to the two different materials. It is important to point out that in actual offshore structures, the joints are expected to experience steel yielding prior to interfacial debonding and/or composite wrap failure. However, preliminary studies showed that, for instance, when upscaling from medium to full-scale joints, the ultimate bond capacity increases 25% less than steel resistance, which might lead to debonding failure in some cases. Therefore, in order to contribute to future design procedures and gather knowledge related to failure associated with interfacial debonding and composite material, the failure envelope generated in this paper concerns only the composite wrap.

3.2 Cohesive Zone Model

In order to simulate the damage on the composite-steel interface, CZM approach was used, and different four-linear traction separation laws were introduced in the model as contact interaction properties (see Fig. 2). The fracture behaviors for pure Mode I and pure Mode II were determined with a basis in previous experiments [6, 7], while intermediate cohesive laws were established through the interpolation of values obtained for pure Mode I and pure Mode II. More information concerning the determination of traction separation laws shapes and values can be found in [6, 7].

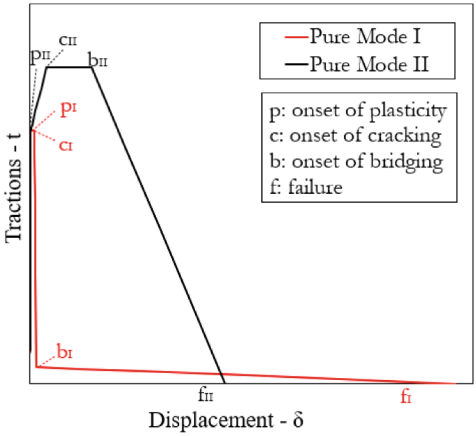

Fig. 2. Traction separation laws for different mode mixity ratios.

3.3 Mesh Elements and Size

Four-node linear tetrahedrons (C3D4) were used to model the composite wrap due to its capacity to simulate complex and curved geometries, while eight-node linear hexahedral elements (C3D8R) were chosen to model the steel chords and braces due to their higher accuracy and more computational efficiency to simulate simpler geometries. After a mesh convergence study, a global mesh size of 4 mm was adopted for the CHS components elements, whereas, for the composite wrap, sizes varying from 4 mm (close to the end of the wrap) up to 16 mm (towards the joint center) were adopted (Fig. 3).

3.4 Boundary Conditions and Load Cases

Six load cases were assessed for three different values of fracture toughness (G_1 = 4.5 N/mm; G_2 = 6 N/mm and G_3 = 7.5 N/mm), including pure axial force (N_x), pure bending out-of-plane moment (M_{op}), and four intermediate bi-axial loading cases with simultaneous application of axial load and bending ($N_x + M_{op}$), as shown in Table 1. The assessed range of fracture toughness was selected based on previous experiments conducted on medium-scale steel-composite coupons [8]. The values were varied by mainly

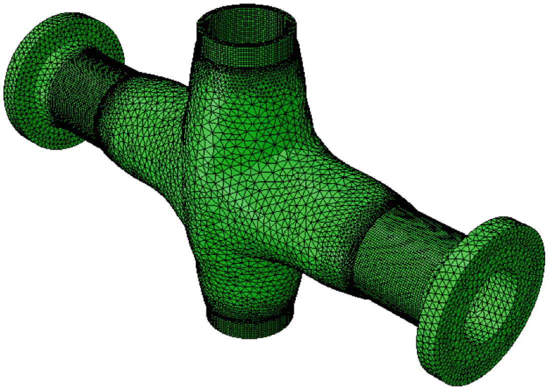

Fig. 3. Mesh configuration for wrapped composite joints.

reducing the interfacial strength and consequently the strain energy release rates (SERR) related to crack tip and fiber bridging in the traction separation laws, for both Mode I, Mode II and intermediate mode mixity ratios. In order to simplify the investigation, only the interaction between axial force and moment-out-of-plane was considered.

Table 1. Assessed multi-axial loading cases.

Loading case	Load combination	Applied F (kN)	Applied M (kN.m)	Assessed fracture toughness (N/mm)
LC1	Nx	1,700	0	$G_1 = 4.5$ $G_2 = 6$ $G_3 = 7.5$
LC2	Nx + Mop	1,500	80	
LC3	Nx + Mop	900	120	
LC4	Nx + Mop	500	150	
LC5	Nx + Mop	200	200	
LC6	Mop	0	200	

The axial force N_x and bending M_{op} were applied symmetrically at the points RP-1 and RP-2, as shown in Fig. 4. The former was applied in the X direction, while the latter was applied around the Y axis. A first attempt at using the common displacement control approach was conducted. However, it resulted in high non-linearity and unclear results in cases where the bending moment is dominant. Therefore, load control was chosen to be used in this work to prevent the introduction of apparently spurious compression in the steel chord due to a prescribed displacement in the X direction. To simulate the boundary conditions and provide stability to the joint, two internal nodes at the joint center were restrained in the Y direction, while 4 nodes (at the bottom and the top of the chord) were restrained in the X and Y directions.

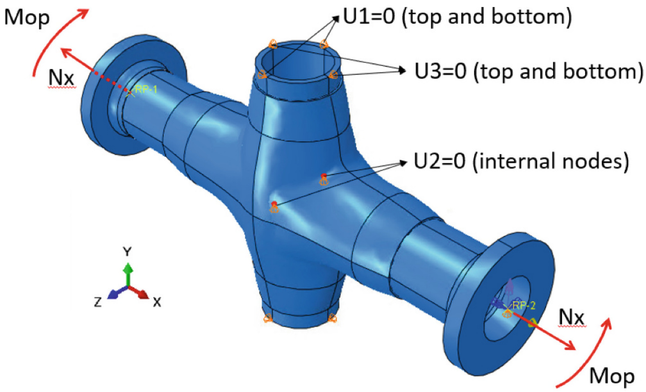

Fig. 4. Load/Moment application and boundary conditions.

4 Results and Discussion

4.1 Failure Modes

Typically, three types of failure modes were observed (see Fig. 5): (a) composite material failure, which is characterized by a diagonal crack on the wrap at one of the braces; (b) complete debonding between composite and steel occurring simultaneously with the emergence of a diagonal crack; (c) complete debonding at one or both of the braces. It was noticed that the fracture toughness value has a significant influence on the debonding progression and, therefore, on the failure mode. For instance, lower values of fracture toughness, such as $G_1 = 4.5$ N/mm and $G_2 = 6$ N/mm, led to a rapid debonding progression between steel and composite, which resulted in a failure mode characterized by the complete debonding at one or two braces for all assessed load cases. On the other hand, for a higher fracture toughness ($G_3 = 7.5$ N/mm), material failure occurred for all bi-axial loading cases (LC2 to LC5) due to retarded progression of steel-composite debonding. For the LC2 case, material failure occurred simultaneously with complete debonding at the brace.

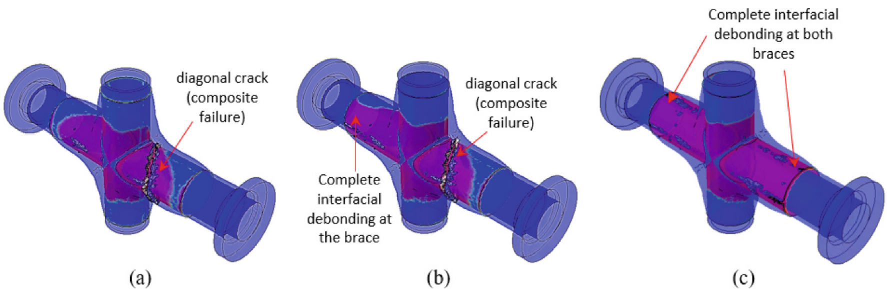

Fig. 5. Failure modes: (a) composite material failure; (b) complete debonding + composite material failure; (c) complete debonding.

4.2 Load vs. Displacement and Moment vs. Rotation Curves

Figures 6, 7 and 8 present the load *vs.* displacement and moment *vs.* rotation curves corresponding to all six assessed loading cases for the three considered fracture toughness. It was noticed that higher fracture toughness leads to a slight improvement in ductile behavior. Moreover, when decreasing by 20% the steel-composite interfacial strength, reductions of approximately 10% and 12% were found for the ultimate axial load and out-of-plane bending moment, respectively. Similarly, decreases of around 20% and 24% were observed in resistant axial force and moment when reducing the fracture toughness by 40%.

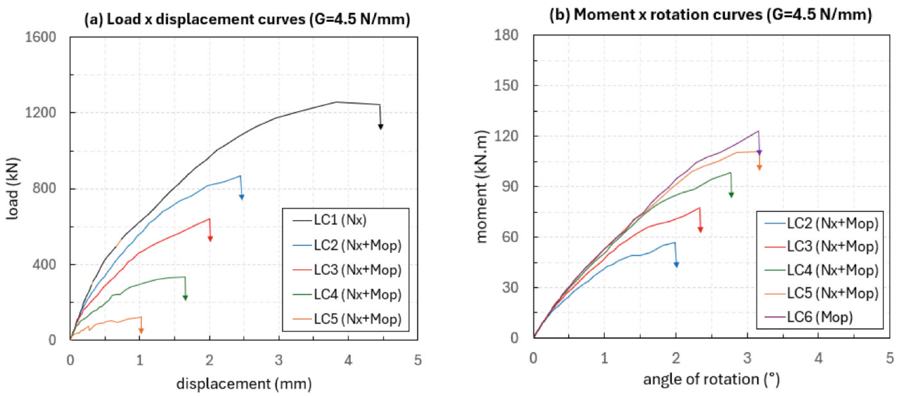

Fig. 6. Numerical curves for $G_1 = 4.5$ N/mm: (a) load *vs.* displacement; (b) moment *vs.* rotation.

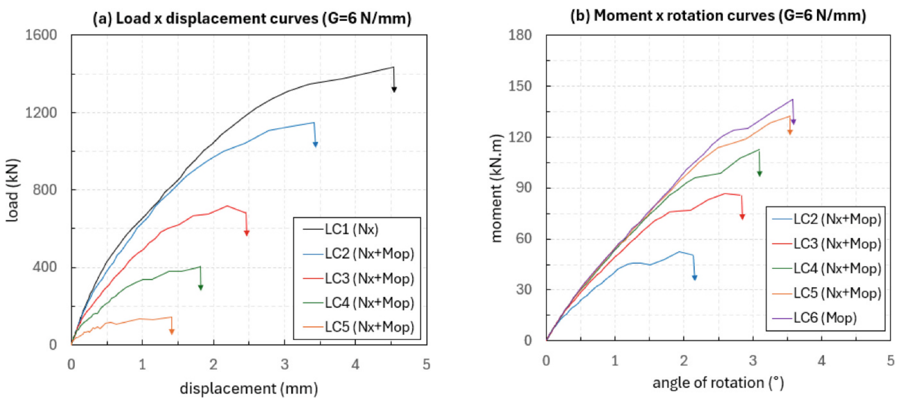

Fig. 7. Numerical curves for $G_2 = 6$ N/mm: (a) load *vs.* displacement; (b) moment *vs.* rotation.

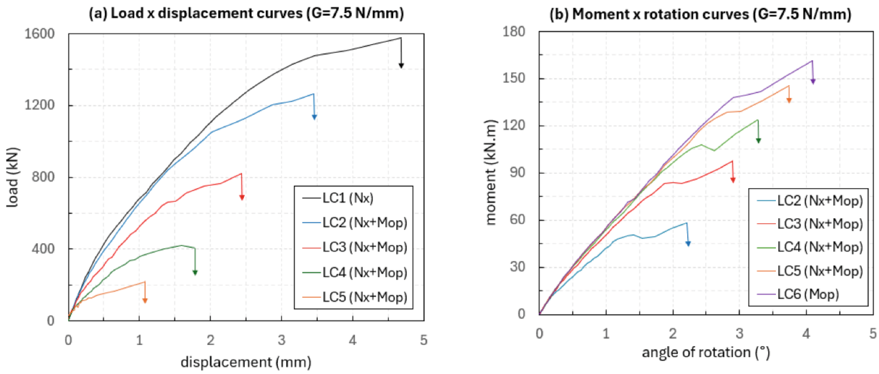

Fig. 8. Numerical curves for $G_3 = 7.5$ N/mm: (a) load *vs.* displacement; (b) moment *vs.* rotation.

4.3 Failure Envelopes and Interaction Exponents

Preliminary analyses were conducted for the multi-axial interaction criterion of wrapped composite joints and have shown that, in cases where axial loads act simultaneously with bending forces, the joint resistance is underestimated when considering a linear summation of the normalized strength values. Therefore, further studies are needed to determine the optimum interaction criterion exponents. Based on existing procedures to determine the multi-axial loading interaction for offshore structures [9, 10], Eq. 1 can be proposed to design the wrapped composite joint subjected to combined axial tension and out-of-plane bending forces.

$$\left(\frac{Nx}{Nx_u}\right)^{\alpha} + \left(\frac{Mop}{Mop_u}\right)^{\beta} \leq 1 \tag{1}$$

Where N_x and M_{op} are the design values for the tensile axial force and moment out-of-plane, respectively, whereas $N_{x,u,}$ and $M_{op,u}$ are the ultimate values for the axial force and out-of-plane bending moment and in-plane bending moment. The parameters α and β are the exponents of the interaction criterion.

2D failure envelopes were obtained from numerical results for three different fracture toughness, as shown in Fig. 9a. The parameters α and β were obtained by non-linear regression, fitting a curve to the numerical data points through the least square method. Figures 9b, c, and d show the comparison between the normalized numerical failure envelope curve, obtained for each fracture toughness, and the given fitted curves (indicated in orange), which were fitted by using the parameters $\alpha = 0.9$ and $\beta = 1.5$. It can be seen that the failure envelopes for G_1, $G_{2,}$ and G_3 presented consistent results between each other, even though different failure modes were observed for $G_3 = 7.5$ N/mm for loading cases LC2 to LC5, as indicated in Fig. 9a. Moreover, the fitted curves agree well with the numerical results by using the same exponents for all three values of fracture toughness.

Therefore, the interaction criteria for axial and out-of-plane bending forces for wrapped composite joints with different fracture toughness parameters can be expressed by Eq. 2. It can be concluded that the given exponents do not seem to be affected by the change in interfacial strength and fracture toughness. This is a valuable conclusion for the development of future design guidelines, especially when taking into account the challenges to obtaining reliable fracture toughness with a basis on fracture mechanics experiments.

$$\left(\frac{Nx}{Nx_u}\right)^{0.9} + \left(\frac{Mop}{Mop_u}\right)^{1.5} \leq 1 \quad (2)$$

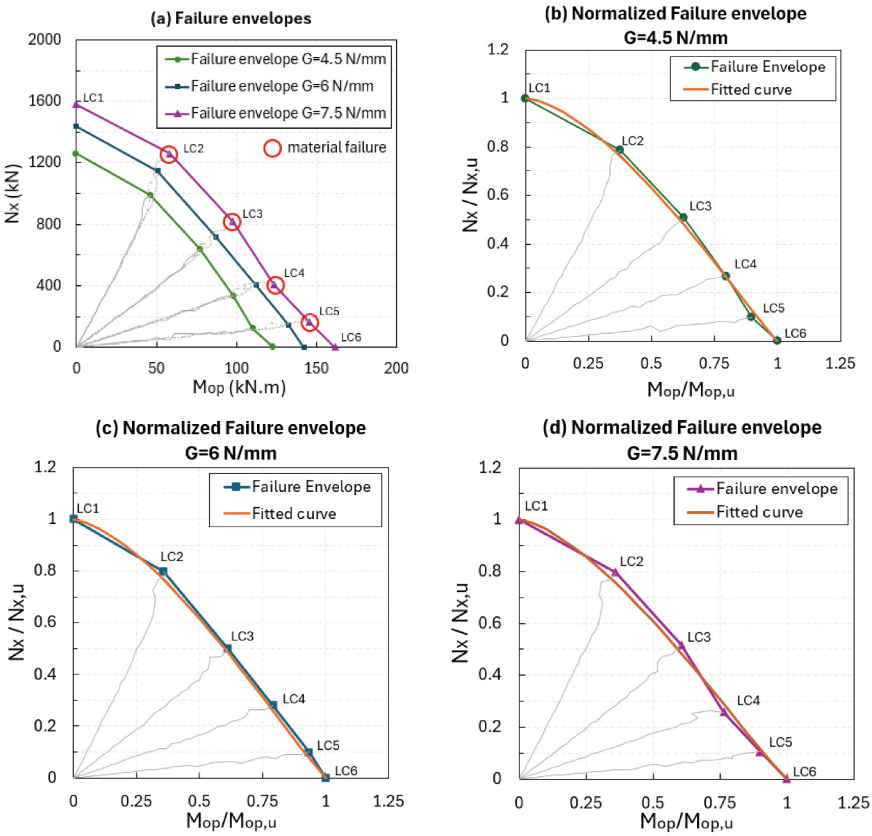

Fig. 9. Failure envelopes: (a) Numerical curves for $G_1 = 4.5$ N/mm, $G_2 = 6$ N/mm and $G_3 = 7.5$ N/mm; (b) Normalized curves for $G_1 = 4.5$ N/mm; (c) Normalized curves for $G_2 = 6$ N/mm; (d) Normalized curves for $G_3 = 7.5$ N/mm.

5 Conclusions

A medium-scale X-shaped wrapped composite joint was simulated in a 3D finite element model based on the CZM approach in order to assess the influence of the fracture toughness on the exponents of the multi-axial loading interaction criterion. Six loading cases were considered to generate 2D failure envelopes corresponding to three different fracture toughnesses. Based on previous standards, a multi-axial loading interaction criterion was proposed, and the following conclusions can be drawn from this work:

- For all loading cases, the joint experiences a progressive debonding between steel and composite materials at the level of chord and braces, before presenting a sudden failure. Concerning the influence of fracture toughness in the failure behavior of wrapped composite joints, it was observed that lower values of fracture toughness led to a prevailing debonding progression between steel and composite, resulting in a complete debonding failure mode. Furthermore, higher fracture toughness led to a slight improvement in the joint ductility.
- Reductions of approximately 10% and 12% were observed, respectively, for the ultimate axial load and the out-of-plane bending moment when decreasing the steel-composite interfacial strength by 20%. Similarly, it was noticed that a reduction of 40% of the fracture toughness led to decreases of around 20% and 24% in resistant axial force and moment.
- The interaction exponents between axial load and out-of-plane bending are not influenced by the fracture toughness of the interface. From an engineering perspective, this implies that variations in interface quality do not impact the governing design check. Furthermore, this represents an important conclusion for future design guidelines, offering a valuable simplification in the calculation procedure, especially when taking into account the challenges to accurately determine fracture toughness with an experimental basis.

Acknowledgments. The authors would like to thank the Rijksdienst voor Ondernemend Nederland (RVO) for the financial support with Topsector Energiesubsidie van het Ministerie van Economische Zaken through WrapNode-II project.

References

1. Pavlovic, M., Veljkovic, M., Segeren, M.: Wrapped composite joints for circular hollow section structures. ce/papers. **6**(3–4), 1179–1184 (2023). https://doi.org/10.1002/cepa.2754
2. He, P., Pavlovic, M.: Failure modes of bonded wrapped composite joints for steel circular hollow sections in ultimate load experiments. Eng. Struct. **254** (2022). https://doi.org/10.1016/j.engstruct.2021.113799
3. Koetsier, M., Yang, J., Pavlovic, M.: Experimental investigation of wrapped composite X-joints under monotonic uniaxial and multi-axial load conditions
4. Smith, M.: ABAQUS/Standard User's Manual. 2009, Dassault Systèmes Simulia Corp.: Version 6.9
5. Feng, W., Arouche, M.M., Pavlovic, M.: Fatigue crack growth characterization of composite-to-steel bonded interface using ENF and 4ENF tests. Compos. Struct. **334**, Article 117963 (2024). https://doi.org/10.1016/j.compstruct.2024.117963
6. He, P., Moreira Arouche, M., Koetsier, M., Pavlovic, M.: Mode I fracture behavior of glass fiber composite-steel bonded interface – experiments and CZM. Compos. Struct. **330**, 117814 (2024). https://doi.org/10.1016/j.compstruct.2023.117814

7. He, P., Koetsier, M., Mylonopoulos, V., Pavlovic, M.: Mode II fracture behavior of glass fiber composite-steel bonded interface–experiments and CZM. Eng. Fract. Mech. **310**, 110510 (2024). https://doi.org/10.1016/j.engfracmech.2024.110510
8. Yang, J., Arouche, M.M., Egilsson, S., Koetsier, M., Peeters, T., Pavlovic, M.: Size effects on mode I and mode II fracture behavior of FRP–steel bonded interface: experimental and numerical investigation. J. Compos. Constr. **29**(2), 04025006 (2025). https://doi.org/10.1061/JCCOF2.CCENG-4760
9. ISO 19902:2020 - Petroleum and natural gas industries — Fixed steel offshore structures (2020)
10. Norwegian Technology Standards Institution, "NORSOK N-004:2013 - Design of Steel Structures," Norway, 2013. [Online]. Available: http://www.nts.no/norsok